Cell Reports
Article

Commensal Microbiota Are Required for Systemic Inflammation Triggered by Necrotic Dendritic Cells

Jennifer A. Young,[1] Tina H. He,[1] Boris Reizis,[2] and Astar Winoto[1,*]
[1]Department of Molecular and Cell Biology and Cancer Research Laboratory, University of California, Berkeley, CA 94720, USA
[2]Department of Microbiology, Columbia University Medical Center, New York, NY 10032, USA
*Correspondence: winoto@berkeley.edu
http://dx.doi.org/10.1016/j.celrep.2013.04.033

SUMMARY

The relationship between dendritic cells (DCs) and commensal microflora in shaping systemic immune responses is not well understood. Here, we report that mice deficient for the Fas-associated death domain in DCs developed systemic inflammation associated with elevated proinflammatory cytokines and increased myeloid and B cells. These mice exhibited reduced DCs in gut-associated lymphoid tissues due to RIP3-dependent necroptosis, whereas DC functions remained intact. Induction of systemic inflammation required DC necroptosis and commensal microbiota signals that activated MyD88-dependent pathways in other cell types. Systemic inflammation was abrogated with the administration of broad-spectrum antibiotics or complete, but not DC-specific, deletion of *MyD88*. Thus, we have identified a previously unappreciated role for commensal microbiota in priming immune cells for inflammatory responses against necrotic cells. These studies demonstrate the impact intestinal microflora have on the immune system and their role in eliciting proper immune responses to harmful stimuli.

INTRODUCTION

Successful immunity relies on the ability of dendritic cells (DCs) to recognize pathogens, secrete inflammatory cytokines, and present antigens to initiate T cell activation (Banchereau et al., 2000). DCs are present in all tissues and survey their environment to induce protection against infectious agents or tolerance to self-antigens. This is particularly important in the intestinal mucosa where DCs constantly encounter microbes and other foreign antigens. The intestinal microenvironment and commensal microbiota interactions help dictate intestinal DC functions, thereby influencing the functions of other immune cell populations (Coombes and Powrie, 2008; Scott et al., 2011). Thus, the strict regulation of DC activities is important in executing proper immune responses. DC development depends on the cytokine fms-like tyrosine receptor kinase 3 ligand (Flt-3L) (Karsunky et al., 2003; McKenna et al., 2000; Waskow et al., 2008), whereas cellular homeostasis in the periphery is maintained by processes like apoptosis to prevent disease development (Kushwah and Hu, 2010). DCs commonly undergo apoptosis following antigen presentation to T cells to limit immune responses. Inhibition of apoptosis in DCs triggers the development of systemic autoimmune disease (Chen et al., 2006; Mabrouk et al., 2008; Stranges et al., 2007).

The adaptor protein Fas-associated death domain (FADD) plays a crucial role downstream of all death receptors in the induction of apoptosis (Yeh et al., 1998; Zhang et al., 1998). The tumor necrosis factor (TNF) superfamily of death receptors, including CD95 (Fas), TNF receptor type I (TNF-RI), and TNF-related apoptosis-inducing ligand receptor (TRAIL-R), initiate cell death by recruiting FADD and the protease caspase-8 into a complex, resulting in a cascade of protease activation and eventual cell death (Strasser et al., 2009; Wilson et al., 2009). More recent studies, however, have focused on an alternative form of cell death, termed necroptosis or programmed necrosis, that can be initiated by death receptor signaling when apoptosis is blocked (Degterev et al., 2005, 2008; Moquin and Chan, 2010). Necroptosis requires the kinase activities of the death domain containing kinase RIP1 and its family member RIP3, which interact through their RIP homotypic interaction motif (Cho et al., 2009; He et al., 2009; Sun et al., 1999). Thus, direct inhibition of the RIP1 kinase activity with a small molecule inhibitor, necrostatin-1 (Nec-1) or targeted deletion of RIP3 can block necroptosis (Degterev et al., 2005, 2008). Recent reports have demonstrated a role for FADD in regulating necroptosis. In the absence of FADD, depending on the tissues being affected, necroptosis occurs and causes detrimental effects including embryonic lethality, lack of T cell proliferation, and intestinal and skin inflammation (Bonnet et al., 2011; Ch'en et al., 2011; Osborn et al., 2010; Welz et al., 2011; Zhang et al., 2011).

Given the critical role of death in regulating DC functions and its subsequent effect in directing immune responses, we sought to examine the function of FADD in DCs. Using DC-specific conditional knockout mice, we found that FADD was essential in limiting DC necroptosis. In the knockout mice, DC numbers were decreased, especially in gut-associated populations, due to uncontrolled DC death. Importantly, the dysregulation of DC death resulted in the appearance of chronic systemic inflammation characterized by increased levels of serum TNF and an

expansion in myeloid and B cells. We further identified a critical role for the intestinal microbiota in the development of inflammatory responses to necroptotic DCs that required MyD88-dependent signals in non-DC cells. Our study uncovers an essential connection between the commensal microbiota and necroptosis-induced inflammation.

RESULTS

Decreased Dendritic Cell Numbers in Gut-Associated Lymphoid Tissues

To better understand the role of FADD in DC homeostasis and effector functions, we generated conditional knockout mice by crossing *CD11c-Cre* transgenic mice to mice containing floxed alleles of *FADD* (Caton et al., 2007; Osborn et al., 2010). These mice (termed dcFADD$^{-/-}$) exhibited a specific loss of FADD protein expression in CD11c^{+}-enriched splenocytes and in-vitro-generated bone-marrow-derived dendritic cell (BMDC) by western blot analysis (Figure 1A). Previous studies have shown that DCs accumulate in the absence of apoptosis, and this subsequently leads to increased lymphocyte activation and autoimmune disease development (Chen et al., 2006; Mabrouk et al., 2008; Stranges et al., 2007). We therefore assessed the DC populations by first examining cell numbers. Unexpectedly, the loss of FADD did not lead to DC accumulation. Instead, a small but significant decrease in the number of CD11c^{hi}MHCII^{+} conventional DCs (cDCs) was detected in the spleen of dcFADD$^{-/-}$ mice compared to littermate control mice (Figure 1B), whereas the number of plasmacytoid dendritic cells (pDC, CD11c^{lo} Siglec-H^{+}B220^{+}) in bone marrow was unchanged (Figure 1B). This result is consistent with the restricted expression of Cre recombinase by CD11c-Cre to the cDC but not the pDC population (Birnberg et al., 2008). We further investigated different subsets of splenic cDCs by examining CD8 and Sirp1α expression. Compared to other DC subsets, the CD8^{+}Sirp1a^{-} DC subset has been identified to efficiently cross-present antigens to CD8^{+} T cells (Shortman and Heath, 2010). In these dcFADD$^{-/-}$ mice, the percentage of CD8^{+}Sirp1a^{-} DCs was diminished, whereas the CD8^{-}Sirp1α^{+} subset was increased (Figure 1C).

Because only a modest decrease in the cDC population was detected in the spleen, we investigated changes in DC numbers in other peripheral lymphoid organs, in particular, the gut-associated lymphoid tissues (GALTs). The mesenteric lymph nodes (MLNs), and Peyer's patches were examined for CD103^{+} migratory DCs (Coombes and Powrie, 2008; Scott et al., 2011). Interestingly, we observed a dramatic reduction of CD103^{+} DCs in the GALT of dcFADD$^{-/-}$ mice compared to the spleen, suggesting that the intestinal microbiota might stimulate DC death (Figure 1D). We subsequently measured the levels of Flt-3L in the serum, because Flt-3L levels have been shown to increase in mice deficient of DCs (Birnberg et al., 2008). We found that Flt-3L was indeed slightly elevated in the sera of dcFADD$^{-/-}$ mice compared to littermate controls (Figure 1E).

The importance of FADD in DC functions was also determined. DCs isolated from the MLNs expressed equivalent levels of MHC and costimulatory molecules (Figure S1). Following stimulation with lipopolysaccharide (LPS), FADD-deficient BMDCs were capable of inducing TNF and IL-12 similar to that of control BMDCs (Figure 1F). Additionally, the ability to stimulate antigen-specific responses by FADD-deficient DCs was evaluated. Proliferation of ovalbumin-specific CD8 T cells (OT-I T cells) in response to ovalbumin peptide (SIINFEKL)-pulsed BMDC was induced in vitro or in vivo. Both control and FADD-deficient BMDCs stimulated OT-I cell proliferation in vitro and in vivo (Figures 1G and 1H). Taking these data together, the deletion of FADD in DCs does not impair their ability to produce cytokines or to initiate T cell responses. However, dcFADD$^{-/-}$ mice exhibit a striking decrease in the number of gut-associated DCs.

Systemic Inflammation in dcFADD$^{-/-}$ Mice Results in Splenomegaly and Lymphadenopathy

The dcFADD$^{-/-}$ mice at first appeared healthy with no obvious abnormalities. However, by 4–8 weeks of age, these mice exhibited splenomegaly and lymphadenopathy compared to littermate controls (Figures 2A and 2B). Increased numbers of Ter119^{+} erythrocytes contributed to the enlargement of the spleens (Figure 2C). In contrast, erythroid cell numbers in the bone marrow of dcFADD$^{-/-}$ mice were lowered compared to their littermate controls (Figure 2C). We also detected elevated B cell numbers in the spleen and lymph nodes of dcFADD$^{-/-}$ mice (Figure 2D; data not shown). However, the absolute numbers of CD3^{+} T cells and the proportion of CD4 and CD8 T cells were similar between littermate controls and dcFADD$^{-/-}$ mice (Figure 2D; data not shown). Strikingly, numerous myeloid cell populations were increased in the spleens of dcFADD$^{-/-}$ mice compared to control mice (Figures 2E–2G). Flow cytometric analysis of splenocytes revealed elevated numbers of inflammatory monocytes (Ly6C^{hi}CD11b^{+}) in dcFADD$^{-/-}$ mice compared to control littermates (Figures 2E and 2F). In addition, the neutrophil population (Ly6C^{lo}Ly6G^{+}CD11b^{+}) in the spleen and blood was also increased (Figures 2E, 2F, and S2A). The numbers of F4/80^{+}CD11b^{+} macrophages were also elevated in dcFADD$^{-/-}$ mice compared to control mice (Figure 2G). Increased numbers of inflammatory monocytes, neutrophils, and macrophages were also detected in the lymph nodes (data not shown). These data reveal that the dcFADD$^{-/-}$ mice display signs of systemic inflammation.

To further assess inflammation in the dcFADD$^{-/-}$ mice, we measured the levels of different proinflammatory cytokines in the serum. A significant increase in basal TNF, interferon (IFN)-γ, and MCP-1 amounts was detected in the serum of dcFADD$^{-/-}$ mice compared to control mice (Figure 2H). In contrast, serum levels of IL-1β were undetectable in both dcFADD$^{-/-}$ and control mice (data not shown). To determine the ramifications of having increased inflammation, control or dcFADD$^{-/-}$ mice were given a low dose of LPS (100 μg) without the sensitizing agent D-galactosamine. Under this condition, most wild-type mice survived (Figure 2I). However, dcFADD$^{-/-}$ mice were unable to recover and died of LPS-induced endotoxic shock within 18 hr (Figure 2I). The levels of proinflammatory cytokine TNF were significantly increased in the sera of dcFADD$^{-/-}$ mice following the injection of LPS (Figure 2J, 40–60 ng/ml). Elevated IL-1β was also detected (Figure S2B) but at lower levels (<1 ng/ml). These results indicate that LPS-stimulated death of dcFADD$^{-/-}$ mice is caused by the lethal effects of elevated proinflammatory cytokines or by TNF-induced lethal systemic inflammation response

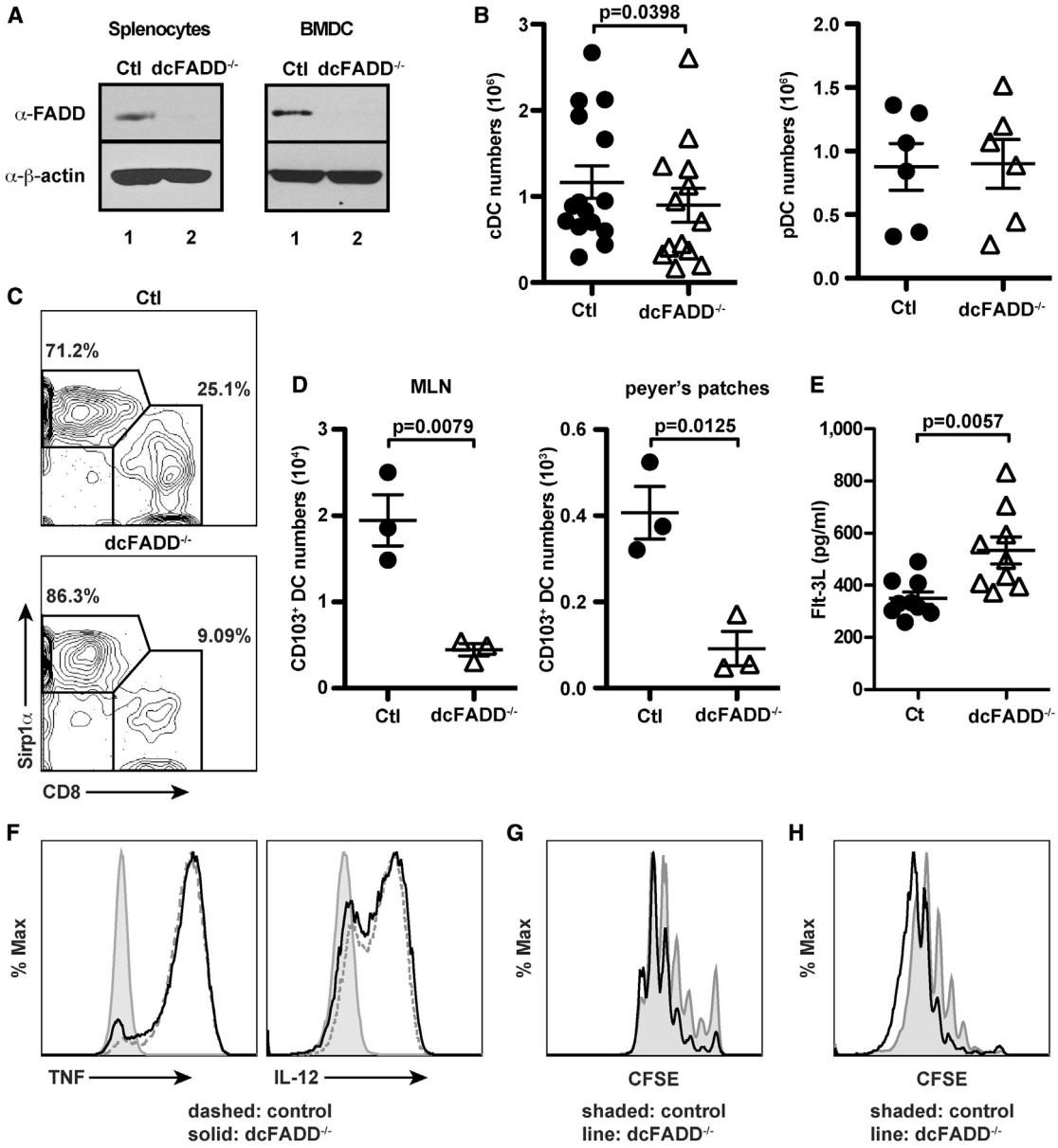

Figure 1. Lower cDC Numbers in dcFADD$^{-/-}$ Mice

(A) FADD protein expression was assessed in CD11c^{+}-enriched splenocytes and BMDCs by western blotting (Ctl, control).

(B) Absolute cell numbers of conventional DCs (cDC: CD11c^{hi}) from the spleen and plasmacytoid DCs (pDC: CD11c^{lo}B220^{+}Siglec H^{+}) from the bone marrow were plotted.

(C) Splenic cDC (CD11c^{hi}MHC II^{+}) subsets were distinguished by CD8 and Sirp1α expression.

(D) Intestinal CD103^{+} DCs in the mesenteric lymph nodes (MLNs) and Peyer's patches were isolated, and cell numbers were calculated.

(E) Flt-3L amounts in the serum were measured by ELISA.

(F) Control (dashed) or dcFADD$^{-/-}$ (solid) BMDCs were stimulated with 10 ng/ml LPS for 6 hr, and intracellular TNF or IL-12 were examined. Histogram plots show cytokine production in CD11c^{+}CD11b^{+} BMDCs. Shaded, unstimulated; dashed, control; solid, dcFADD$^{-/-}$.

(G) CFSE-labeled OT-I cells were cultured with SIINFEKL-pulsed BMDCs (shaded, control; solid line, dcFADD$^{-/-}$) for 72 hr, and OT-I T cell proliferation was measured.

(H) CFSE-labeled OT-I cells were adoptively transferred into β2 m$^{-/-}$ mice, and SIINFEKL-pulsed BMDCs (shaded, control; solid line, dcFADD$^{-/-}$) were injected into the footpad 24 hr later. Seventy-two hours after BMDC injections, the draining popliteal lymph nodes were harvested to examine T cell proliferation. Histograms are representative of duplicate samples and two separate experiments (G and H).

Data are representative of at least three independent experiments (A–F). Plots show mean ± SEM, and each point represents an individual animal (B, D, and E). See also Figure S1.

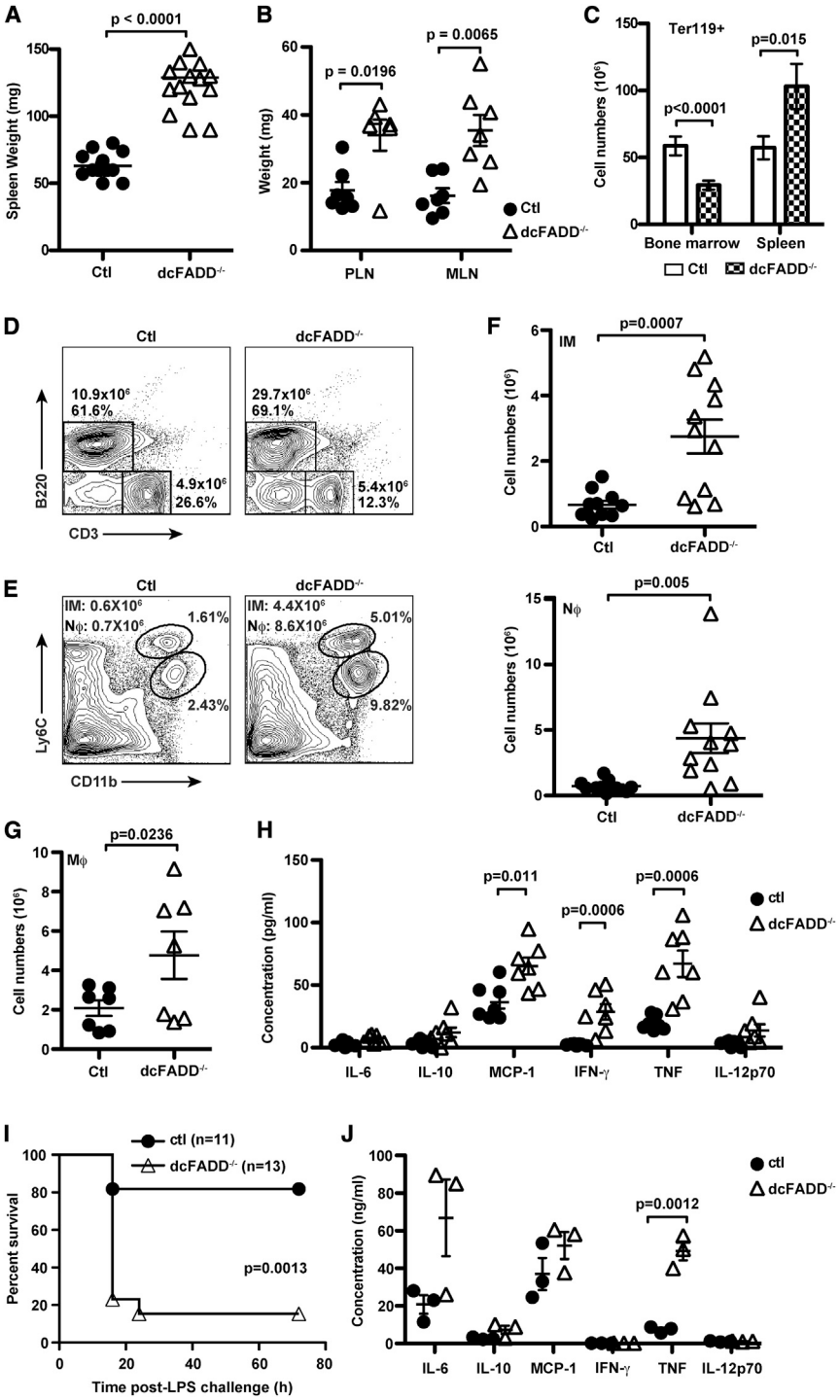

Figure 2. dcFADD$^{-/-}$ Mice Exhibit Systemic Inflammation and Increased Sensitivity to LPS Endotoxic Shock

(A and B) Weights of spleens (A), peripheral (PLN), or mesenteric (MLN) lymph nodes (B) from Ctl or dcFADD$^{-/-}$ mice.

(C) Numbers of Ter119^{+} erythroid in the spleen or bone marrow of Ctl (white bars) or dcFADD$^{-/-}$ (hatched bars) mice (n = 10 for bone marrow, n = 8 for spleen).

(D) CD3 and B220 staining to examine splenic B and T lymphocyte populations. Numbers represent total cell numbers and cell percentages. Data are representative of five separate experiments.

(E) Flow cytometric analysis of inflammatory monocyte (IM: Ly6C^{hi}CD11b^{+}) and neutrophil (Nϕ: Ly6C^{lo}Ly6G^{+}CD11b^{+}) populations in the spleen. Plots are representative of more than five independent experiments.

(F and G) Numbers of IM (F, upper panel), Nϕ (F, lower panel), and macrophages (G, Mϕ: F4/80^{+}CD11b^{+}) in the spleen.

(H) Serum cytokine levels (pg/ml) were measured by flow cytometry using cytometric bead array (CBA) (n = 7).

(I) Ctl (circles, n = 11) or dcFADD$^{-/-}$ (triangles, n = 13) mice were injected with 100 μg of LPS i.p., and survival was compared.

(J) One hour after LPS injections, the amounts of serum cytokines (ng/ml) were measured by CBA.

Bar graph and scatterplots represents mean ± SEM. Each point represents an individual animal and pooled from multiple analyses (A, B, F–H, and J). See also Figure S2.

syndrome (Duprez et al., 2011). Although there are some similarities to mice that completely lack cDCs (Birnberg et al., 2008; Ohnmacht et al., 2009), the dcFADD$^{-/-}$ mice exhibit numerous unique phenotypes. Our data specifically demonstrate that dcFADD$^{-/-}$ mice develop systemic inflammation characterized by elevated levels of proinflammatory cytokines and increased numbers of inflammatory monocyte, neutrophils, macrophages, and B cells. As a consequence, this increased inflammation enhances sensitivity to LPS-induced endotoxic shock.

RIP3-Dependent Necroptosis Is Responsible for DC Death and Systemic Inflammation

We next determined the reason for the reduction in DC numbers, and whether the decrease in DCs was responsible for the systemic inflammation observed in the dcFADD$^{-/-}$ mice. Necroptosis has been described to occur in the absence of apoptosis and requires the kinase activities of RIP1 and RIP3 (Cho et al., 2009; He et al., 2009; Sun et al., 1999). We hypothesized that the lowered DC numbers in dcFADD$^{-/-}$ mice was the result of FADD-deficient DCs dying by necroptosis. Therefore, we first assessed the ability of FADD-deficient DCs to undergo necroptosis in response to Toll-like receptor (TLR) stimulation. BMDCs generated from dcFADD$^{-/-}$ or control mice were stimulated with LPS, and cell death was examined by labeling cells with Annexin V and 7AAD. LPS stimulation induced necroptotic

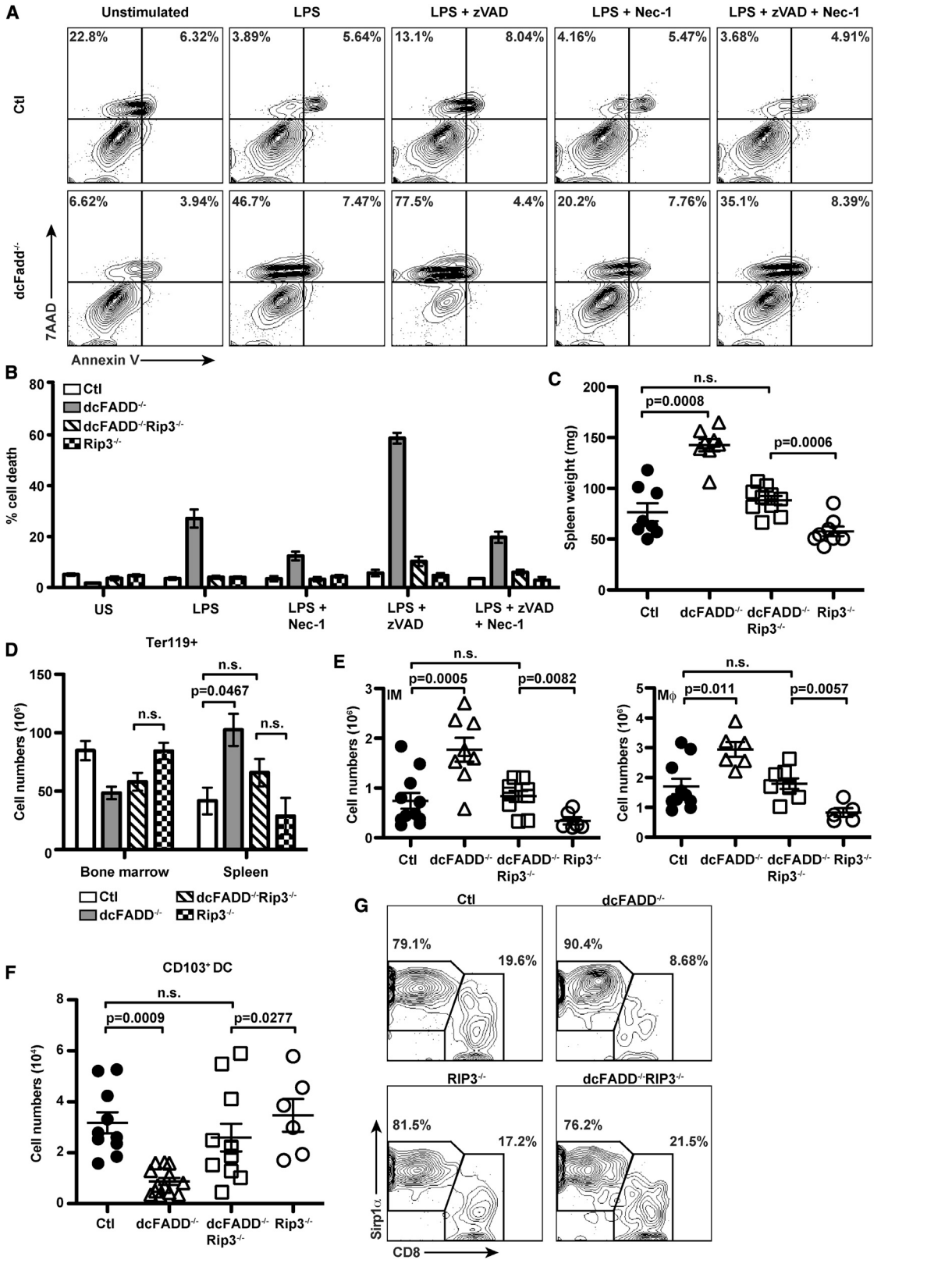

(legend on next page)

cell death (7AAD$^+$/Annexin V$^-$) in FADD-deficient DCs that was not detected in control cells (Figure 3A). Addition of zVAD, a pan-caspase inhibitor, in combination with LPS further increased cell death in both wild-type and FADD-deficient DCs (Figure 3A). Because zVAD blocks apoptosis by inhibiting caspase-8 activity, this result suggested the presence of an alternative caspase-dependent but FADD-independent pathway to death. Interestingly, LPS-induced cell death was only partially rescued by the RIP1 kinase inhibitor Nec-1, implying that LPS stimulated some cells to die by a RIP1-independent manner (Figure 3A).

Necrotic cell death was reported to induce IL-1 release and to promote inflammation (Rock et al., 2010). Following LPS stimulation, increased death of dcFADD$^{-/-}$ cells corresponded with elevated levels of mature IL-1β, whereas the induction of TNF was similar between FADD-deficient and control cells (Figures S3A–S3C). Inflammatory contents released by necrotic cells can trigger potassium efflux, resulting in NLRP3 inflammasome activation and IL-1 processing (Pétrilli et al., 2007). Inhibition of potassium efflux from cells prevented IL-1β production in dcFADD$^{-/-}$ DCs without altering the amount of cell death (Figure S3D and S3E). These data demonstrate that LPS-stimulated dcFADD$^{-/-}$ DCs can undergo necroptosis in vitro and release processed IL-1β.

To further assess necroptosis in DCs, we crossed dcFADD$^{-/-}$ mice to *RIP3*$^{-/-}$ mice to generate dcFADD$^{-/-}$RIP3$^{-/-}$ double-knockout (DKO) mice. BMDCs were generated from dcFADD$^{-/-}$RIP3$^{-/-}$ mice, and necroptosis was measured following LPS stimulation. As mentioned above, LPS-stimulated death of FADD-deficient DCs was only partially rescued by Nec-1 (Figures 3A and 3B). However, the deletion of *RIP3* completely rescued LPS-induced death (Figure 3B). These data demonstrate that in the absence of FADD, DCs can undergo RIP1-dependent and -independent necroptosis, both of which are dependent on RIP3. In contrast, DC death following TNF treatment was completely rescued by Nec-1, suggesting that programmed necrosis induced by TNF is dependent on both RIP1 and RIP3 (Figure S4A).

We subsequently investigated the role of RIP3-dependent necroptosis in the development of systemic inflammation in dcFADD$^{-/-}$ mice. Strikingly, much of the inflammatory phenotypes detected in the dcFADD$^{-/-}$ mice were abrogated in the dcFADD$^{-/-}$RIP3$^{-/-}$ mice. The significant increase in spleen weight seen in dcFADD$^{-/-}$ mice was no longer observed in dcFADD$^{-/-}$RIP3$^{-/-}$ DKO mice, nor was there a difference in the erythrocyte populations (Figures 3C and 3D). Furthermore, the increased numbers of inflammatory monocytes, neutrophils, and macrophages observed in the dcFADD$^{-/-}$ mice were not detected in dcFADD$^{-/-}$RIP3$^{-/-}$ DKO mice (Figures 3E and S4B). Although a slight increase in these myeloid populations was detected in the dcFADD$^{-/-}$RIP3$^{-/-}$ DKO mice compared to *RIP3*$^{-/-}$ mice, no statistical differences were detected between DKO mice and control mice (Figures 3E and S4B). Normal numbers of myeloid cell populations correlated with decreased levels of inflammatory cytokines in the sera of dcFADD$^{-/-}$RIP3$^{-/-}$ DKO mice (Figure S4C; data not shown).

Because the deletion of *RIP3* in FADD-deficient cells prevented necroptotic death in vitro (Figure 3B), we expected that DC numbers would be rescued in dcFADD$^{-/-}$RIP3$^{-/-}$ mice. As shown in Figure 3F, similar numbers of CD103$^+$ migratory DCs were detected in the MLNs of dcFADD$^{-/-}$RIP3$^{-/-}$ DKO and control mice (Figure 3F). Thus, *RIP3* deletion prevented FADD-deficient CD103$^+$ DCs from dying. The deletion of *RIP3* in dcFADD$^{-/-}$ mice also rescued the proportions of CD8$^+$ and Sirp1α$^+$ DC subsets (Figure 3G). Consequently, Flt-3L levels in the serum of dcFADD$^{-/-}$RIP3$^{-/-}$ DKO mice were similar to control and *RIP3*$^{-/-}$ mice (Figure S4D). Furthermore, expression of costimulatory molecules was not affected by the absence of RIP3 (Figure S4E). Together, these results indicate an obligatory role for RIP3 in dcFADD$^{-/-}$ DC death, and this RIP3-dependent death stimulates the development of systemic inflammation in vivo.

MyD88-Dependent Signaling in DCs and Non-DCs Is Crucial for Inflammation in dcFADD$^{-/-}$ Mice

In the absence of FADD, DCs died by necroptosis when stimulated with LPS or other TLR ligands as shown above. Therefore, we hypothesized that reduced DC numbers in the GALT of dcFADD$^{-/-}$ mice could be a consequence of necroptosis induced by TLR ligands presented by commensal microflora. Necroptotic DC death may then release DAMPs (Danger Associated Molecular Patterns proteins) capable of activating other innate cells, resulting in inflammation (Kono and Rock, 2008). MyD88 is an adaptor molecule for IL-1R and most TLRs (Barton and Medzhitov, 2003; Beutler and Rietschel, 2003). To assess the role MyD88 plays in the dcFADD$^{-/-}$ phenotype, we crossed dcFADD$^{-/-}$ mice to *MyD88*$^{flox/flox}$ mice to generate dcFADD$^{-/-}$dcMyD88$^{-/-}$ mice, which specifically deleted both *FADD* and *MyD88* in the DC population. When we examined the dcFADD$^{-/-}$dcMyD88$^{-/-}$ mice for inflammation, an increase in

Figure 3. RIP3 Deletion Prevents DC Necroptosis and Systemic Inflammation

(A) Control (Ctl, upper panels) and dcFADD$^{-/-}$ (lower panels) BMDCs were pretreated with either 10 μM zVAD, 30 μM Nec-1, or DMSO and then stimulated with 10 ng/ml LPS for 16 hr. Cells were labeled with Annexin V and 7AAD. Data are representative of at least five experiments.

(B) Ctl (white bars), dcFADD$^{-/-}$ (gray bars), dcFADD$^{-/-}$RIP3$^{-/-}$ (diagonal bars), and *RIP3*$^{-/-}$ (hatched bars) BMDCs were stimulated, and cell death was measured as in (A) (US, unstimulated). Bar graph shows mean percentage of death ± SEM (percentage 7AAD$^+$/Annexin V$^-$) and representative of at least three individual experiments.

(C) Spleen weights from Ctl, dcFADD$^{-/-}$, dcFADD$^{-/-}$RIP3$^{-/-}$, or *RIP3*$^{-/-}$ mice.

(D) Ter119$^+$ erythroid cells in the spleen and bone marrow (Ctl, white bars, n = 5); dcFADD$^{-/-}$ (gray bars, n = 3); dcFADD$^{-/-}$RIP3$^{-/-}$ (diagonal bars, n = 5); or *RIP3*$^{-/-}$ (hatched bars, n = 4).

(E and F) Number of inflammatory monocyte (IM) and macrophage (Mϕ) in the spleen (E) and CD103$^+$ DCs in the MLN (F).

(G) DC subsets in the spleen were assessed by gating on CD11c^{hi}MHCII$^+$ cDCs and examining CD8 and Sirp1α expression. Numbers are cell percentages, and plots are representative of three independent experiments.

Scatterplots represents mean ± SEM (n.s., not significant). Each point represents an individual animal and pooled from multiple analyses (C–F). See also Figures S3 and S4.

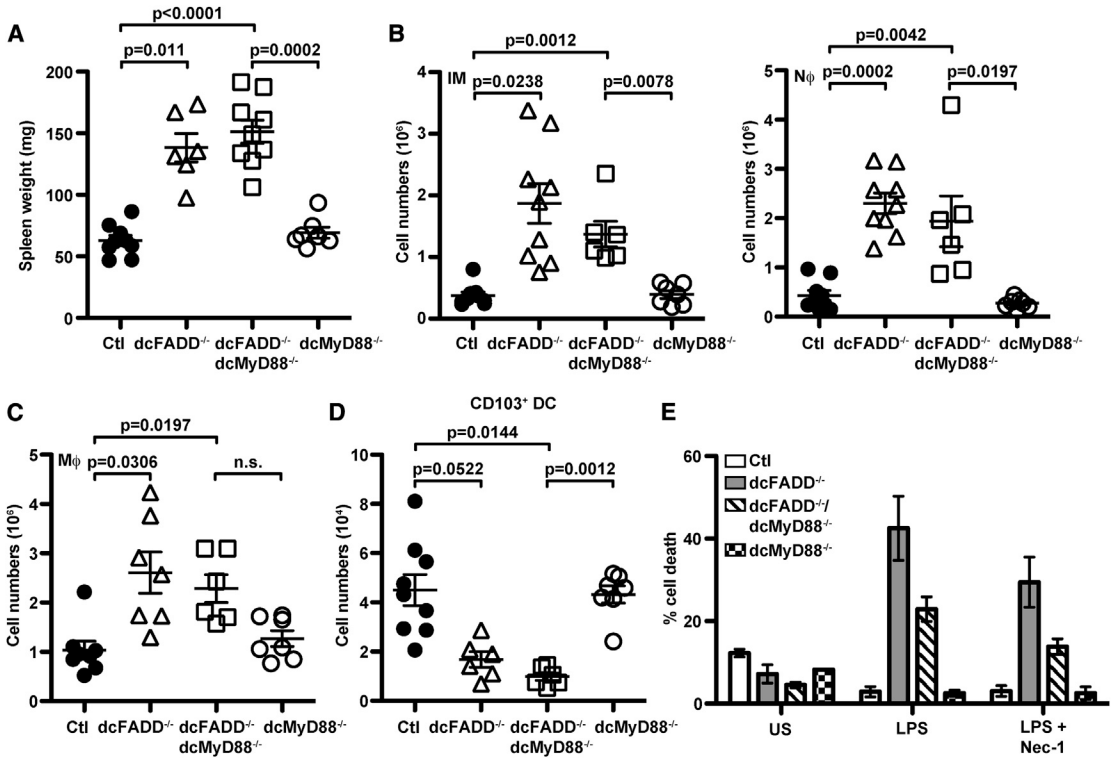

Figure 4. Deletion of MyD88 in DCs Does Not Prevent Death but Partially Rescues dcFADD$^{-/-}$ Phenotypes

(A) Spleen weights from control (Ctl), dcFADD$^{-/-}$, dcFADD$^{-/-}$dcMyD88$^{-/-}$, or dcMyD88$^{-/-}$ mice.

(B and C) Numbers of inflammatory monocytes, neutrophils (B, IM and Nϕ), and macrophages (C) in the spleen.

(D) CD103^{+} DC numbers in the MLN.

(E) BMDCs generated from control (white bars), dcFADD$^{-/-}$ (gray bars), dcFADD$^{-/-}$dcMyD88$^{-/-}$ (diagonal bars), and dcMyD88$^{-/-}$ (hatched bars) mice were pretreated with 30 μM Nec-1, or DMSO and then stimulated with 10 ng/ml LPS for 16 hr and labeled with Annexin V and 7AAD to measure cell death (US, unstimulated).

Bar graphs plotted as mean percentage of death ± SEM and are representative of three individual experiments. Scatterplots represents mean ± SEM (n.s., not significant). Each point represents an individual animal and pooled from multiple analyses (A–D). See also Figure S5.

the spleen weights was still observed (Figure 4A). However, a partial rescue in the numbers of inflammatory monocytes, neutrophils, and macrophages was detected, suggesting a reduction in the levels of inflammation (Figures 4B and 4C). These myeloid populations were reduced in dcFADD$^{-/-}$dcMyD88$^{-/-}$ mice compared to dcFADD$^{-/-}$ mice but slightly increased when compared to control or dcMyD88$^{-/-}$ mice (Figures 4B and 4C). When the CD103^{+} DC population was examined, cell numbers were significantly decreased in dcFADD$^{-/-}$dcMyD88$^{-/-}$ mice compared to control or dcMyD88$^{-/-}$ mice (Figure 4D). Despite the dramatic reduction of DCs in the MLNs, cells deficient of FADD and MyD88 were capable of upregulating MHC and costimulatory molecules (Figure S5). LPS stimulation of FADD- and MyD88-double-deficient BMDCs still induced death when compared to MyD88-deficient cells, although the percentage of death was slightly lower than in FADD-deficient cells (Figure 4E). These results suggest that MyD88-dependent signaling has a role in the initiation of necroptotic death in FADD-deficient DCs in vitro but is not essential in vivo. Commensal bacteria may still stimulate DC death through the TLR4 adaptor molecule TRIF, which has been previously shown to interact with RIP3 to initiate necroptosis (He et al., 2011).

Because we observed a partial rescue of the systemic inflammation in dcFADD$^{-/-}$dcMyD88$^{-/-}$ mice, we investigated whether MyD88 signaling was necessary in other cells types. Interactions between commensal bacteria and host cells rely on MyD88-dependent signals to elicit innate immune responses and to maintain intestinal homeostasis (Hooper et al., 2012). Therefore, to further examine the importance of MyD88 in the development of inflammation, we crossed dcFADD$^{-/-}$ mice to complete *MyD88*$^{-/-}$ knockout mice to generate dcFADD$^{-/-}$MyD88$^{-/-}$ DKO mice. In these mice, *MyD88* was deleted from all cell populations. These mice revealed a dramatically marked decrease in spleen size and weight, such that organ weights were similar to control mice (Figure 5A). Furthermore, the erythrocyte population in the spleen was reduced to wild-type numbers in the dcFADD$^{-/-}$MyD88$^{-/-}$ DKO mice when compared to dcFADD$^{-/-}$ mice (Figure 5B). The B cell population in the DKO mice was also reduced and resembled the numbers observed in *MyD88*$^{-/-}$ controls (Figure 5C). Additionally, the myeloid cell populations (inflammatory monocytes, neutrophils, and macrophages) in the dcFADD$^{-/-}$MyD88$^{-/-}$ mice also returned to similar cell numbers as control mice (Figure 5D). Accordingly, the elevated levels of TNF in dcFADD$^{-/-}$

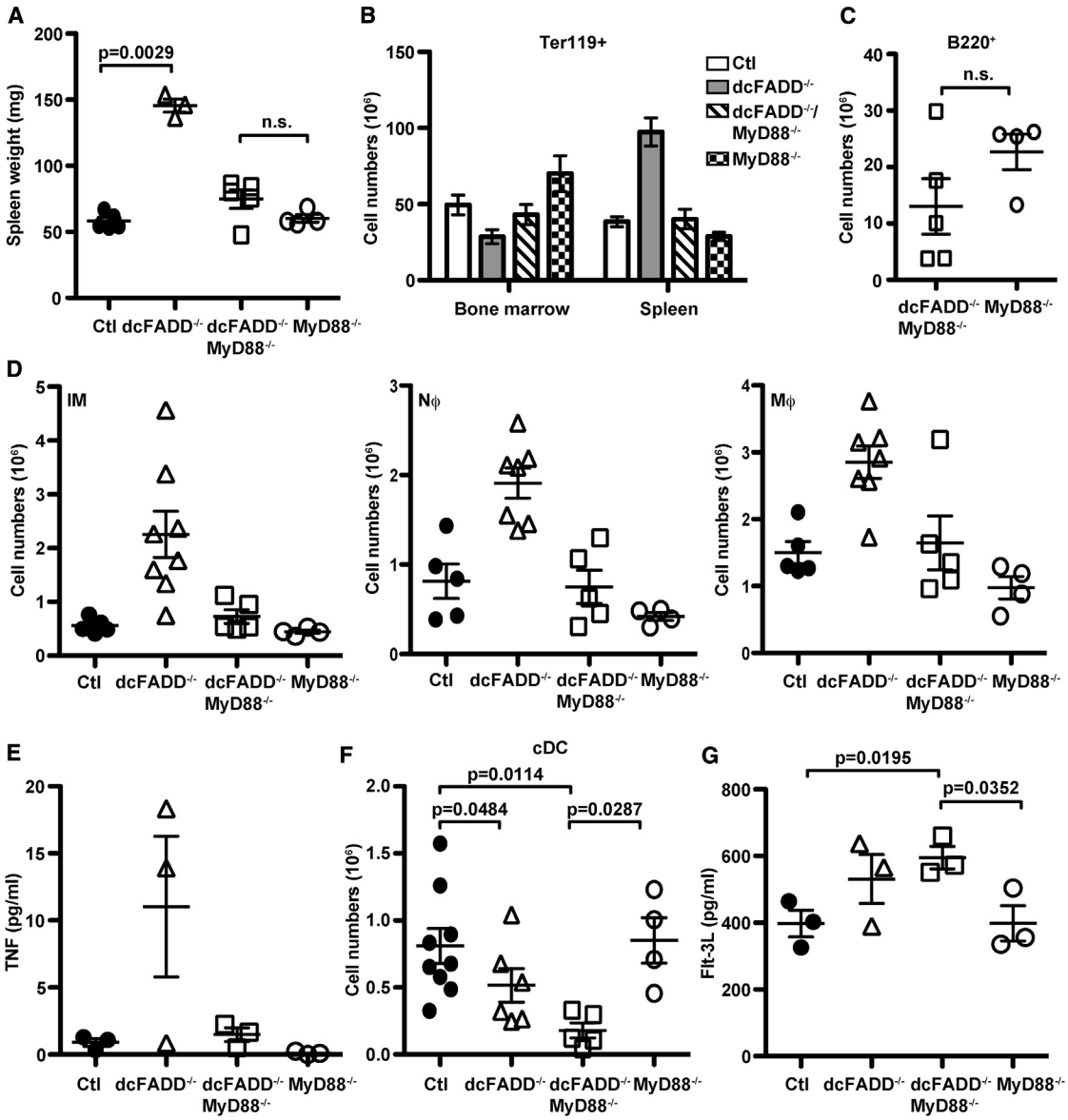

Figure 5. MyD88-Dependent Signaling Is Required for the Development of Inflammation in dcFADD$^{-/-}$ Mice

(A) Weights of spleens from control (Ctl), dcFADD$^{-/-}$, dcFADD$^{-/-}$MyD88$^{-/-}$, or *MyD88*$^{-/-}$ mice.

(B) Ter119^{+} erythroid cells in the spleen and bone marrow (Ctl, white bars, n = 5); dcFADD$^{-/-}$ (gray bars, n = 3); dcFADD$^{-/-}$MyD88$^{-/-}$ (diagonal bars, n = 5); *MyD88*$^{-/-}$ (hatched bars, n = 4).

(C and D) Absolute numbers of B220^{+} B cell (C), inflammatory monocyte, neutrophil, and macrophage (D, IM, Nϕ, and Mϕ, respectively) in the spleen.

(E) TNF levels (pg/ml) in the serum were measured by ELISA.

(F) Splenic DCs (CD11c^{hi}MHC II^{+}) numbers were measured and plotted.

(G) The levels of serum Flt-3L were measured by ELISA.

Scatterplots represents mean ± SEM (n.s., not significant). Each point represents an individual animal pooled from multiple analyses (A and C–G).

mice were lowered to wild-type amounts in dcFADD$^{-/-}$MyD88$^{-/-}$ mice (Figure 5E). Similar to results with dcFADD$^{-/-}$dcMyD88$^{-/-}$ mice, complete deletion of *MyD88* did not rescue DC numbers (Figure 5F). The DCs in dcFADD$^{-/-}$MyD88$^{-/-}$ DKO mice were significantly decreased compared to the numbers of DCs detected in control and *MyD88*$^{-/-}$ mice (Figure 5F). The diminished DC numbers in dcFADD$^{-/-}$MyD88$^{-/-}$ DKO mice also correlated with elevated Flt-3L amounts (Figure 5G). These results demonstrate that MyD88 is not necessary for the reduction in the cDC population. In the absence of MyD88, DCs still die by necroptosis. However, MyD88 is required for the development of inflammation observed in dcFADD$^{-/-}$ mice. Thus, MyD88-dependent signaling in populations other than DCs is surprisingly crucial for the development of systemic inflammation in response to DC necroptosis.

Systemic Inflammation in dcFADD$^{-/-}$ Mice Is Abrogated by Antibiotic Treatment

A potential explanation for the requirement of MyD88 in the development of inflammation is that the commensal microflora signals through MyD88-dependent pathways, which "primes" cells for DAMP-induced inflammation. The appreciable decrease of CD103^{+} migratory DCs in the GALT and the absence of systemic inflammation in dcFADD$^{-/-}$MyD88$^{-/-}$ mice supported a role for commensal bacteria (Figures 1D and 5). To eliminate most of the commensal microflora, we treated 2-day-old mice with a broad spectrum of antibiotics for 4–5 weeks. Following antibiotic treatment, dcFADD$^{-/-}$ and control mice had similar-sized spleens and MLNs (Figure 6A). Furthermore, antibiotic treatment reduced the number of inflammatory monocytes, neutrophils, macrophages, and B cells in dcFADD$^{-/-}$ mice (Figures 6B and 6C). Therefore, the systemic inflammation observed in untreated dcFADD$^{-/-}$ mice was rescued in antibiotic-treated animals. In support of the MyD88 data, results from the antibiotic treatments validate the contribution of intestinal microbiota to the systemic inflammation in dcFADD$^{-/-}$ mice. Thus, the signals generated from necroptotic DCs alone are insufficient to trigger the development of inflammation.

DISCUSSION

The analysis of mice with FADD-deficient DCs has allowed us to investigate the importance of FADD in dendritic cell death, the effect of necroptotic death on the immune response, and the role of commensal bacteria on different immune cell populations. FADD deficiency sensitized cells to necrotic death leading to decreased DCs in mice. In contrast to FADD-deficient T cells that are nonfunctional (Osborn et al., 2010; Zhang et al., 2011), FADD-deficient DCs were able to secrete cytokines and induced antigen-specific T cell responses. Additionally, dcFADD$^{-/-}$ mice had a heightened state of systemic inflammation, which was different from other tissue-specific FADD-deficient mice that exhibited localized inflammation (Bonnet et al., 2011; Welz et al., 2011). It is surprising that death of a proportion of dendritic cells in the GALT was capable of driving system-wide effects. Deletion of *RIP3* in dcFADD$^{-/-}$ mice rescued DC death and also decreased systemic inflammation to normal levels, suggesting DC necroptosis is responsible for all the dcFADD$^{-/-}$ mouse phenotype. However, without assessing DC-specific RIP3-deficient mice, we cannot exclude the formal possibility of *RIP3* deletion in other cell types playing a role as well. Blocking signals from commensal microbiota with MyD88 deficiency in all cell populations also abrogated systemic inflammation in dcFADD$^{-/-}$ mice. These experiments describe not only a role for FADD in preventing necroptosis in DCs, but also demonstrate a role for commensal bacteria in an inflammatory response against necroptotic cells, which presumably release inflammation-inducing molecules.

Necroptosis is a form of cell death initially described to be downstream of the death receptors requiring RIP1 and RIP3 interaction and their kinase activities (Cho et al., 2009; He et al., 2009). FADD-deficient DCs were more sensitive to cell death in response to TLR stimulation in vitro. In vivo, FADD-deficient DCs presumably died from stimulation by commensal microflora. We found that LPS-induced death of dcFADD$^{-/-}$ cells was only partially inhibited by Nec-1 but completely blocked in the absence of RIP3. Conversely, TNF-stimulated death was completely rescued by Nec-1 treatment. These data suggest that TLR4 can induce both a RIP1/RIP3-dependent death and a RIP3-dependent but RIP1-independent death. The RIP1/RIP3-dependent death can potentially be mediated by upregulation of TNF by TLR signaling, in turn signaling through the TNF-RI to induce RIP1-dependent necroptosis. RIP1-independent and RIP3-dependent death may be initiated directly downstream of TLR4 as previously described by other groups (He et al., 2011; Upton et al., 2010, 2012). In FADD-deficient DCs, RIP3-dependent necroptosis is likely linked to the adaptor protein TRIF downstream of TLR4. TRIF is a known adaptor protein that can associate with TLR4 or TLR3, receptors for LPS and poly(I:C), respectively (Yamamoto et al., 2002). Indeed, dcFADD$^{-/-}$dcMyD88$^{-/-}$ BMDCs still died when stimulated with LPS. In this case, FADD may serve as a negative inhibitor of the TRIF-RIP3 complex.

The absence of FADD in other cell types also caused marked sensitivity to necroptosis (Bonnet et al., 2011; Osborn et al., 2010; Welz et al., 2011; Zhang et al., 2011). Similarly, caspase-8 deficiency exhibited the same sensitivity to RIP3-dependent programmed necrosis (Ch'en et al., 2011; Günther et al., 2011; Kaiser et al., 2011; Oberst et al., 2011). Interestingly, during the writing of this manuscript, a report showed that LPS alone did not stimulate necroptotic death in caspase-8-deficient DCs (Casp8^{-}) (Kang et al., 2013). This is in contrast to FADD-deficient DCs, which exhibit exacerbated death upon LPS stimulation. In addition, ATP release from dying cells likely stimulates IL-1β production by dcFADD$^{-/-}$ cells. Potassium treatment diminished IL-1β levels, implying a role for potassium efflux and the NLRP3 inflammasome (Pétrilli et al., 2007). In addition, there are unique phenotypes in the dcFADD$^{-/-}$ mice not observed in Casp8^{-} mice. For instance, fewer DC numbers were observed in dcFADD$^{-/-}$ mice, whereas Casp8^{-} mice exhibited unaltered or increased DC numbers. Increased macrophage and B cell populations with augmented TNF levels were observed in dcFADD$^{-/-}$ but not Casp8^{-} mice. The difference in necroptosis execution in FADD and caspase-8 DC models highlights the critical role FADD plays in cell death. Caspase-8/RIP3 DKO mice suffered from T and B cell autoimmunity at an early age, marked by an increase of the signature CD3^{+}B220^{+} population and elevated levels of ANA. Preliminary results indicate that 6-week-old dcFADD$^{-/-}$RIP3$^{-/-}$ mice also exhibited elevated number of CD3^{+}B220^{+} double-positive cells, but no antinuclear antibodies were detected (data not shown). It remains to be seen whether aged dcFADD$^{-/-}$RIP3$^{-/-}$ will have an accumulation of cDCs and develop systemic autoimmunity.

Some phenotypes in dcFADD$^{-/-}$ mice, including the expansion of monocytes, neutrophils, and erythrocytes in the spleen, as well as decreased red blood cells in the bone marrow, were similar to what was observed in mice lacking cDCs, also known as DC-less mice (Birnberg et al., 2008; Ohnmacht et al., 2009). Flt-3L had been shown to control homeostasis of DCs in the bone marrow and periphery (Hochweller et al., 2009; McKenna et al., 2000) and was thought to be the main culprit for the phenotype of DC-less mice. The receptor kinase Flt-3 is critical in DC

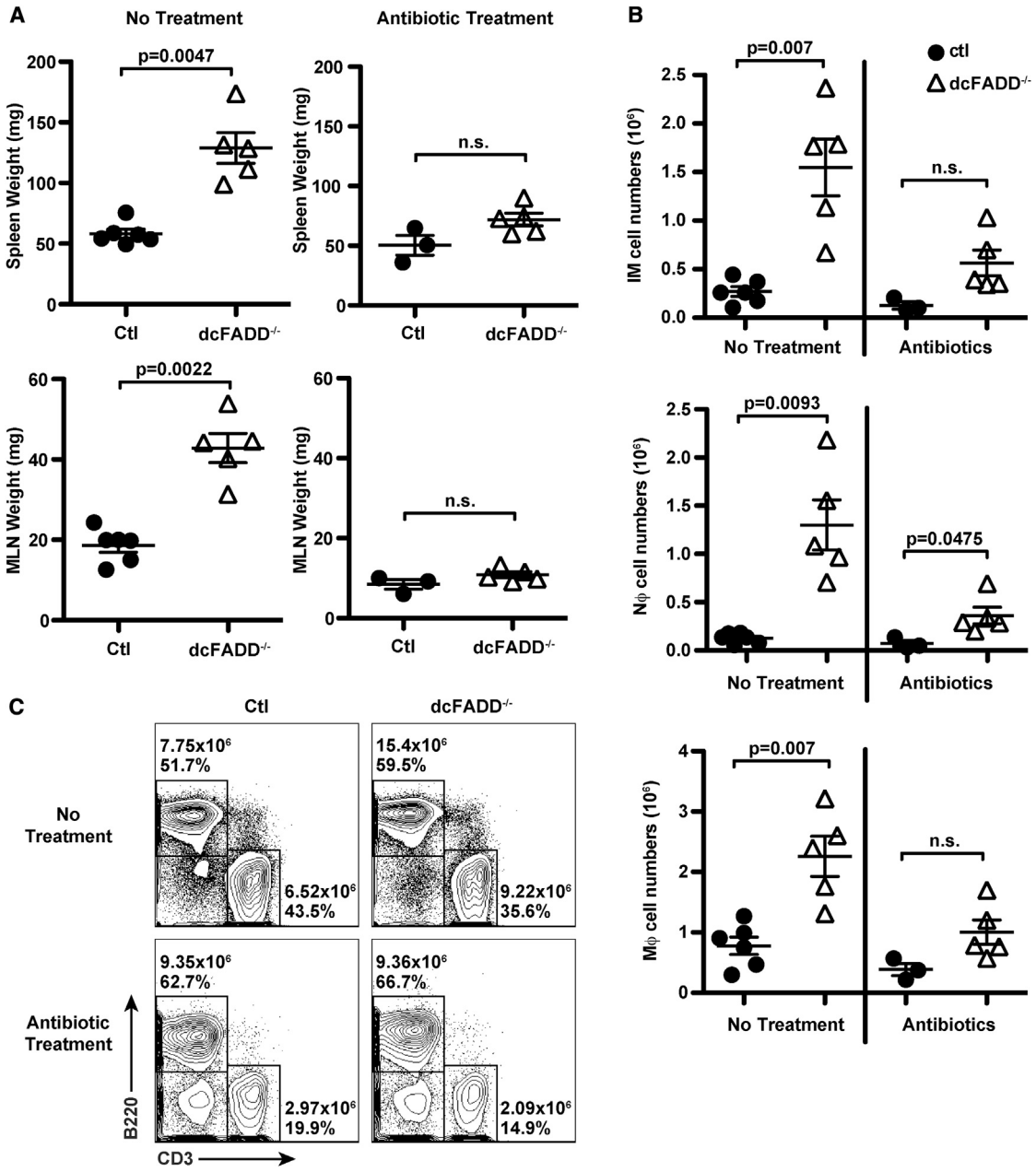

Figure 6. Treatment with Broad-Spectrum Antibiotics Rescues Systemic Inflammation in dcFADD$^{-/-}$ Mice

Mice were treated with a cocktail of antibiotics in the drinking water from day 2 of birth until the time of analysis (at 4–5 weeks of age).

(A) Spleen (upper panels) and MLN (lower panels) weights from nontreated (no treatment, left panels) and antibiotic-treated (right panels) mice were measured.

(B) Absolute numbers of inflammatory monocytes (IM), neutrophils (Nϕ), and macrophages (Mϕ) in the spleen.

(C) B220^{+} and CD3^{+} lymphocyte populations in the spleen of nontreated (upper panels) or antibiotic-treated (lower panels) mice were analyzed (Ctl mice, left panels; dcFADD$^{-/-}$ mice, right panels).

Numbers represent total cell numbers and cell percentages. Scatterplots represents mean ± SEM, and each point represents an individual animal (n.s., not significant). Data are representative of three separate experiments (A–C).

development and is expressed on common myeloid progenitors and differentiated DCs (Karsunky et al., 2003; Waskow et al., 2008). In previous reports on DC-less mice, the increased Flt-3L levels compensating for the changes in cell homeostasis led to myeloproliferative disease and erythrocyte imbalance (Birnberg et al., 2008). The decreased DC numbers in the spleen and GALT were sufficient to induce a moderate increase in Flt-3L. The ability of Flt-3L to expand the progenitor population allows for the repopulation of DCs in the periphery (Hochweller et al., 2009; Karsunky et al., 2003; Waskow et al., 2008). Thus,

elevated serum levels of Flt-3L in dcFADD$^{-/-}$ mice may continually differentiate progenitor cells into DCs, thereby dampening the reduction in splenic cDC numbers. However, in contrast to DC-less mice, dcFADD$^{-/-}$ mice also exhibited elevated levels of TNF and other cytokines as well as higher numbers of macrophages and B cells. Increased Flt-3L in the serum is not likely to be the main reason for increased myeloid and erythrocyte populations in dcFADD$^{-/-}$ mice. Consistent with this, serum levels of Flt-3L were elevated in dcFADD$^{-/-}$MyD88$^{-/-}$ mice, but the inflammatory phenotype of dcFADD$^{-/-}$ mice were not exhibited.

The role of MyD88-dependent signals in the induction of inflammation was examined by crossing dcFADD$^{-/-}$ mice with *MyD88*$^{-/-}$ mice. The absence of MyD88 did not rescue the death of DCs in dcFADD$^{-/-}$ mice. However, the inflammatory phenotype in dcFADD$^{-/-}$ mice was completely absent in dcFADD$^{-/-}$MyD88$^{-/-}$ mice. On the other hand, specific deletion of *MyD88* in the DC population only partially rescued the phenotype exhibited by dcFADD$^{-/-}$ mice. In this case, TLR signaling was defective in only a small proportion of cells, whereas MyD88-dependent signals remained intact in other cell populations. Although MyD88-dependent signals were not necessary for DC death, these data suggested that signaling through MyD88 was required for most of the inflammatory phenotypes observed in dcFADD$^{-/-}$ mice. MyD88 is an essential adaptor for signaling through TLRs and IL-1/18 receptors (Barton and Medzhitov, 2003; Beutler and Rietschel, 2003). In previous reports, IL-1 signaling was responsible for the inflammation induced by necrotic cells, thus *MyD88*$^{-/-}$ mice failed to recruit neutrophils in response to dead cells (Rock et al., 2010). Stimulation of FADD-deficient cells produced increased amounts of IL-1β in vitro, which implies that IL-1β could contribute to the inflammation detected in dcFADD$^{-/-}$ mice. However, the levels of IL-1β were undetectable in dcFADD$^{-/-}$ mice. Therefore, IL-1β does not appear to play a significant role in the inflammation in dcFADD$^{-/-}$ mice, and the absence of inflammatory responses in the dcFADD$^{-/-}$MyD88$^{-/-}$ mice is the outcome of defective TLR signaling.

TLR ligands from commensal microflora are likely the source of "tonic signals" which prime cells to respond to DAMPs. Closer examination of the migratory DCs from the gut revealed a greater decrease in this DC subset, suggesting a role for intestinal microbiota. Administration of broad-spectrum antibiotics rescued the inflammatory phenotypes in dcFADD$^{-/-}$ mice. These data supported a role for MyD88-dependent signaling in the development of inflammation. Intestinal DCs constantly survey the gut microbiota in order to maintain intestinal homeostasis. At the same time, the intestinal microflora can influence immune responses by stimulating MyD88 signaling pathways in various cell populations (Hooper et al., 2012). For example, productive antiviral immune responses have been reported to depend on the presence of commensal bacteria (Abt et al., 2012; Ichinohe et al., 2011). One explanation for needing intestinal microflora in immunity is that gut commensals provide signals to prime immune cells for activation, and indeed macrophages isolated from antibiotic-treated mice are less responsive to viral stimulation (Abt et al., 2012). Therefore, a potential model for the dcFADD$^{-/-}$ mice may be that commensal microbiota provide MyD88-dependent signals that prime myeloid and B cells to respond to inflammatory stimuli. Activation of primed myeloid/B cells by necroptotic FADD-deficient DCs then elicits an inflammatory response. In the absence of commensal-generated signals, either by antibiotic treatment or by *MyD88* deletion, stimulation from necroptotic DCs alone is not sufficient to induce inflammation. Thus, our studies uncover a critical relationship between commensal microbiota and the ability of innate immune cells and B cells to respond to necroptotic cells. In addition, we found that dysregulation of DC necroptosis at intestinal sites can drive systemic inflammation. More importantly, these data demonstrate that commensal microbiota are necessary for a functional immune system to respond to danger signals coming from pathogens or cellular stress.

EXPERIMENTAL PROCEDURES

Mice

Mice were used at 6–12 weeks of age unless otherwise noted. Littermates or sex- and age-matched (within 10 days) mice were used as controls. dcFADD$^{-/-}$ mice were generated by crossing *CD11c-Cre* transgenic mice with *FADD*^{flox} mice. Mice containing FADD alleles floxed with loxP sites were generated in the lab and backcrossed to C57BL/6 for at least ten generations (Osborn et al., 2010). *CD11c-Cre* mice have been previously described (Caton et al., 2007). *MyD88*$^{-/-}$ mice (in C57BL/6 background) were provided by Dr. Shizuo Akira (Adachi et al., 1998) through Dr. Greg Barton, and *RIP3*$^{-/-}$ mice (backcrossed to C57BL/6 for more than eight generations) were from Dr. Xiaodong Wang (He et al., 2009). *MyD88*^{flox} mice (Hou et al., 2008) were purchased from The Jackson Laboratory. For antibiotic treatment, mice were fed a cocktail of 1 mg/ml ampicillin, 1 mg/ml neomycin, 0.5 mg/ml ciprofloxacin, and 0.5 mg/ml meropenem in the drinking water flavored with 20 mg/ml grape Kool-Aid from day 2 of birth. Following weaning, mice maintained on the same antibiotic cocktail except with 0.5 mg/ml vancomycin in place of ciprofloxacin until analysis (Welz et al., 2011). Mice treated with antibiotics were analyzed between 4 and 5 weeks of age. All experiments utilized cohoused mice. Experimental mice were housed in the animal facility at the University of California, Berkeley, and all procedures involving animals were approved by the Animal Care and Use Committee.

Dendritic Cell Enrichment

To isolate splenic DCs, spleens were cut into small pieces, digested with collagenase IV (GIBCO) at 37°C for 35 min, and then incubated with 25 mM EDTA for 5 min at room temperature before dissociating and filtering cells through a 100 μm strainer. CD11c^{+} DCs were enriched using CD11c magnetic particles (Miltenyi Biotec) according to manufacturer's instructions.

Bone marrow was flushed from femurs and tibias using a needle and syringe. Red blood cells were lysed, and 2 × 10^{6} BM cells were cultured in 10 cm non-tissue-culture-treated dishes in complete RPMI-1640 supplemented with 10% FCS, L-glutamine, penicillin-streptomycin, sodium pyruvate, 2-mercaptoethanol, and granulocyte macrophage colony-stimulating factor (GMCSF) (collected supernatant from X63-GMCSF cell line (Zal et al., 1994), a generous gift of Dr. Brigitta Stockinger at National Institute for Medical Research, London through Dr. Tomasc Zal at Scripps). Cells were cultured for 8–10 days with fresh media added on days 3, 6, and 8. BMDCs were harvested and replated in complete RPMI with or without GMCSF for stimulation. Alternatively, CD11c^{+} BMDCs were purified with magnetic particles.

ELISA and Cytometric Bead Array

Blood was collected from tail vein or cardiac puncture, and different proteins in the serum were analyzed by sandwich ELISA. The levels of Flt3L (R&D Systems), TNF-α, and IL-1β (ebioscience) were determined using ELISA kits. Additionally, multiple cytokines were quantitated with the mouse inflammation cytometric bead array kit (BD Biosciences). Samples were collected on the LSR II and analyzed with FCAP Array Software (BD Biosciences).

Cell Death Induction

To examine cell death in dendritic cells, cells were pretreated with 10 μM zVAD-FMK and/or 30 μM necrostatin-1 for 30 min and then stimulated with 10 ng/ml LPS or 100 ng/ml recombinant TNF-α at 37°C. Following 16–18 hr of stimulation, BMDCs were harvested in cold PBS and surface stained with anti-CD11c and anti-CD11b in fluorescence-activated cell sorting buffer. Cells were then washed in Annexin V binding buffer and labeled with fluorescein isothiocyanate-Annexin V and 7AAD. Samples were analyzed by flow cytometry.

Statistical Analysis

Statistical significance was calculated using paired or unpaired Student's t test. Mann-Whitney U test was used to compare survival curves. Statistical analysis was completed with GraphPad Prism (GraphPad). For reagents and additional method details, please refer to the Extended Experimental Procedures.

SUPPLEMENTAL INFORMATION

Supplemental Information includes Extended Experimental Procedures and five figures and can be found with this article online at http://dx.doi.org/10.1016/j.celrep.2013.04.033.

LICENSING INFORMATION

ACKNOWLEDGMENTS

We thank S. He and Xiaodong Wang for the generous gift of *RIP3*$^{-/-}$ mice and M. Koch, H. Melichar, G. Barton, and E. Robey for sharing mice and reagents and for helpful discussions. We are grateful to A. Chuang and Y.F. Sun for technical help and Hector Nolla for support with flow cytometry. We thank J. Halkias, J. Coombes, and S. Nandu for critical reading of the manuscript and helpful discussions. This work was funded by NIH grants PO1 AI065831 (Project 2) and RO1 AI095299 (to A.W.) and NIH training grants T32 CA009179-32 and T32 CA009041-35 (to J.A.Y.).

Received: December 21, 2012
Revised: April 9, 2013
Accepted: April 29, 2013
Published: May 30, 2013

REFERENCES

Abt, M.C., Osborne, L.C., Monticelli, L.A., Doering, T.A., Alenghat, T., Sonnenberg, G.F., Paley, M.A., Antenus, M., Williams, K.L., Erikson, J., et al. (2012). Commensal bacteria calibrate the activation threshold of innate antiviral immunity. Immunity *37*, 158–170.

Adachi, O., Kawai, T., Takeda, K., Matsumoto, M., Tsutsui, H., Sakagami, M., Nakanishi, K., and Akira, S. (1998). Targeted disruption of the MyD88 gene results in loss of IL-1- and IL-18-mediated function. Immunity *9*, 143–150.

Banchereau, J., Briere, F., Caux, C., Davoust, J., Lebecque, S., Liu, Y.J., Pulendran, B., and Palucka, K. (2000). Immunobiology of dendritic cells. Annu. Rev. Immunol. *18*, 767–811.

Barton, G.M., and Medzhitov, R. (2003). Toll-like receptor signaling pathways. Science *300*, 1524–1525.

Beutler, B., and Rietschel, E.T. (2003). Innate immune sensing and its roots: the story of endotoxin. Nat. Rev. Immunol. *3*, 169–176.

Birnberg, T., Bar-On, L., Sapoznikov, A., Caton, M.L., Cervantes-Barragán, L., Makia, D., Krauthgamer, R., Brenner, O., Ludewig, B., Brockschnieder, D., et al. (2008). Lack of conventional dendritic cells is compatible with normal development and T cell homeostasis, but causes myeloid proliferative syndrome. Immunity *29*, 986–997.

Bonnet, M.C., Preukschat, D., Welz, P.S., van Loo, G., Ermolaeva, M.A., Bloch, W., Haase, I., and Pasparakis, M. (2011). The adaptor protein FADD protects epidermal keratinocytes from necroptosis in vivo and prevents skin inflammation. Immunity *35*, 572–582.

Caton, M.L., Smith-Raska, M.R., and Reizis, B. (2007). Notch-RBP-J signaling controls the homeostasis of CD8- dendritic cells in the spleen. J. Exp. Med. *204*, 1653–1664.

Ch'en, I.L., Tsau, J.S., Molkentin, J.D., Komatsu, M., and Hedrick, S.M. (2011). Mechanisms of necroptosis in T cells. J. Exp. Med. *208*, 633–641.

Chen, M., Wang, Y.H., Wang, Y., Huang, L., Sandoval, H., Liu, Y.J., and Wang, J. (2006). Dendritic cell apoptosis in the maintenance of immune tolerance. Science *311*, 1160–1164.

Cho, Y.S., Challa, S., Moquin, D., Genga, R., Ray, T.D., Guildford, M., and Chan, F.K. (2009). Phosphorylation-driven assembly of the RIP1-RIP3 complex regulates programmed necrosis and virus-induced inflammation. Cell *137*, 1112–1123.

Coombes, J.L., and Powrie, F. (2008). Dendritic cells in intestinal immune regulation. Nat. Rev. Immunol. *8*, 435–446.

Degterev, A., Huang, Z., Boyce, M., Li, Y., Jagtap, P., Mizushima, N., Cuny, G.D., Mitchison, T.J., Moskowitz, M.A., and Yuan, J. (2005). Chemical inhibitor of nonapoptotic cell death with therapeutic potential for ischemic brain injury. Nat. Chem. Biol. *1*, 112–119.

Degterev, A., Hitomi, J., Germscheid, M., Ch'en, I.L., Korkina, O., Teng, X., Abbott, D., Cuny, G.D., Yuan, C., Wagner, G., et al. (2008). Identification of RIP1 kinase as a specific cellular target of necrostatins. Nat. Chem. Biol. *4*, 313–321.

Duprez, L., Takahashi, N., Van Hauwermeiren, F., Vandendriessche, B., Goossens, V., Vanden Berghe, T., Declercq, W., Libert, C., Cauwels, A., and Vandenabeele, P. (2011). RIP kinase-dependent necrosis drives lethal systemic inflammatory response syndrome. Immunity *35*, 908–918.

Günther, C., Martini, E., Wittkopf, N., Amann, K., Weigmann, B., Neumann, H., Waldner, M.J., Hedrick, S.M., Tenzer, S., Neurath, M.F., and Becker, C. (2011). Caspase-8 regulates TNF-α-induced epithelial necroptosis and terminal ileitis. Nature *477*, 335–339.

He, S., Wang, L., Miao, L., Wang, T., Du, F., Zhao, L., and Wang, X. (2009). Receptor interacting protein kinase-3 determines cellular necrotic response to TNF-alpha. Cell *137*, 1100–1111.

He, S., Liang, Y., Shao, F., and Wang, X. (2011). Toll-like receptors activate programmed necrosis in macrophages through a receptor-interacting kinase-3-mediated pathway. Proc. Natl. Acad. Sci. USA *108*, 20054–20059.

Hochweller, K., Miloud, T., Striegler, J., Naik, S., Hämmerling, G.J., and Garbi, N. (2009). Homeostasis of dendritic cells in lymphoid organs is controlled by regulation of their precursors via a feedback loop. Blood *114*, 4411–4421.

Hooper, L.V., Littman, D.R., and Macpherson, A.J. (2012). Interactions between the microbiota and the immune system. Science *336*, 1268–1273.

Hou, B., Reizis, B., and DeFranco, A.L. (2008). Toll-like receptors activate innate and adaptive immunity by using dendritic cell-intrinsic and -extrinsic mechanisms. Immunity *29*, 272–282.

Ichinohe, T., Pang, I.K., Kumamoto, Y., Peaper, D.R., Ho, J.H., Murray, T.S., and Iwasaki, A. (2011). Microbiota regulates immune defense against respiratory tract influenza A virus infection. Proc. Natl. Acad. Sci. USA *108*, 5354–5359.

Kaiser, W.J., Upton, J.W., Long, A.B., Livingston-Rosanoff, D., Daley-Bauer, L.P., Hakem, R., Caspary, T., and Mocarski, E.S. (2011). RIP3 mediates the embryonic lethality of caspase-8-deficient mice. Nature *471*, 368–372.

Kang, T.B., Yang, S.H., Toth, B., Kovalenko, A., and Wallach, D. (2013). Caspase-8 blocks kinase RIPK3-mediated activation of the NLRP3 inflammasome. Immunity *38*, 27–40.

Karsunky, H., Merad, M., Cozzio, A., Weissman, I.L., and Manz, M.G. (2003). Flt3 ligand regulates dendritic cell development from Flt3+ lymphoid and

myeloid-committed progenitors to Flt3+ dendritic cells in vivo. J. Exp. Med. *198*, 305–313.

Kono, H., and Rock, K.L. (2008). How dying cells alert the immune system to danger. Nat. Rev. Immunol. *8*, 279–289.

Kushwah, R., and Hu, J. (2010). Dendritic cell apoptosis: regulation of tolerance versus immunity. J. Immunol. *185*, 795–802.

Mabrouk, I., Buart, S., Hasmim, M., Michiels, C., Connault, E., Opolon, P., Chiocchia, G., Lévi-Strauss, M., Chouaib, S., and Karray, S. (2008). Prevention of autoimmunity and control of recall response to exogenous antigen by Fas death receptor ligand expression on T cells. Immunity *29*, 922–933.

McKenna, H.J., Stocking, K.L., Miller, R.E., Brasel, K., De Smedt, T., Maraskovsky, E., Maliszewski, C.R., Lynch, D.H., Smith, J., Pulendran, B., et al. (2000). Mice lacking flt3 ligand have deficient hematopoiesis affecting hematopoietic progenitor cells, dendritic cells, and natural killer cells. Blood *95*, 3489–3497.

Moquin, D., and Chan, F.K. (2010). The molecular regulation of programmed necrotic cell injury. Trends Biochem. Sci. *35*, 434–441.

Oberst, A., Dillon, C.P., Weinlich, R., McCormick, L.L., Fitzgerald, P., Pop, C., Hakem, R., Salvesen, G.S., and Green, D.R. (2011). Catalytic activity of the caspase-8-FLIP(L) complex inhibits RIPK3-dependent necrosis. Nature *471*, 363–367.

Ohnmacht, C., Pullner, A., King, S.B., Drexler, I., Meier, S., Brocker, T., and Voehringer, D. (2009). Constitutive ablation of dendritic cells breaks self-tolerance of CD4 T cells and results in spontaneous fatal autoimmunity. J. Exp. Med. *206*, 549–559.

Osborn, S.L., Diehl, G.E., Han, S.-J., Xue, L., Kurd, N., Hsieh, K., Cado, D., Robey, E.A., and Winoto, A. (2010). Fas-associated death domain (FADD) is a negative regulator of T-cell receptor-mediated necroptosis. Proc. Natl. Acad. Sci. USA *107*, 13034–13039.

Pétrilli, V., Papin, S., Dostert, C., Mayor, A., Martinon, F., and Tschopp, J. (2007). Activation of the NALP3 inflammasome is triggered by low intracellular potassium concentration. Cell Death Differ. *14*, 1583–1589.

Rock, K.L., Latz, E., Ontiveros, F., and Kono, H. (2010). The sterile inflammatory response. Annu. Rev. Immunol. *28*, 321–342.

Scott, C.L., Aumeunier, A.M., and Mowat, A.M. (2011). Intestinal CD103+ dendritic cells: master regulators of tolerance? Trends Immunol. *32*, 412–419.

Shortman, K., and Heath, W.R. (2010). The CD8+ dendritic cell subset. Immunol. Rev. *234*, 18–31.

Stranges, P.B., Watson, J., Cooper, C.J., Choisy-Rossi, C.M., Stonebraker, A.C., Beighton, R.A., Hartig, H., Sundberg, J.P., Servick, S., Kaufmann, G., et al. (2007). Elimination of antigen-presenting cells and autoreactive T cells by Fas contributes to prevention of autoimmunity. Immunity *26*, 629–641.

Strasser, A., Jost, P.J., and Nagata, S. (2009). The many roles of FAS receptor signaling in the immune system. Immunity *30*, 180–192.

Sun, X., Lee, J., Navas, T., Baldwin, D.T., Stewart, T.A., and Dixit, V.M. (1999). RIP3, a novel apoptosis-inducing kinase. J. Biol. Chem. *274*, 16871–16875.

Upton, J.W., Kaiser, W.J., and Mocarski, E.S. (2010). Virus inhibition of RIP3-dependent necrosis. Cell Host Microbe *7*, 302–313.

Upton, J.W., Kaiser, W.J., and Mocarski, E.S. (2012). DAI/ZBP1/DLM-1 complexes with RIP3 to mediate virus-induced programmed necrosis that is targeted by murine cytomegalovirus vIRA. Cell Host Microbe *11*, 290–297.

Waskow, C., Liu, K., Darrasse-Jèze, G., Guermonprez, P., Ginhoux, F., Merad, M., Shengelia, T., Yao, K., and Nussenzweig, M. (2008). The receptor tyrosine kinase Flt3 is required for dendritic cell development in peripheral lymphoid tissues. Nat. Immunol. *9*, 676–683.

Welz, P.S., Wullaert, A., Vlantis, K., Kondylis, V., Fernández-Majada, V., Ermolaeva, M., Kirsch, P., Sterner-Kock, A., van Loo, G., and Pasparakis, M. (2011). FADD prevents RIP3-mediated epithelial cell necrosis and chronic intestinal inflammation. Nature *477*, 330–334.

Wilson, N.S., Dixit, V., and Ashkenazi, A. (2009). Death receptor signal transducers: nodes of coordination in immune signaling networks. Nat. Immunol. *10*, 348–355.

Yamamoto, M., Sato, S., Mori, K., Hoshino, K., Takeuchi, O., Takeda, K., and Akira, S. (2002). Cutting edge: a novel Toll/IL-1 receptor domain-containing adapter that preferentially activates the IFN-beta promoter in the Toll-like receptor signaling. J. Immunol. *169*, 6668–6672.

Yeh, W.-C., Pompa, J.L., McCurrach, M.E., Shu, H.-B., Elia, A.J., Shahinian, A., Ng, M., Wakeham, A., Khoo, W., Mitchell, K., et al. (1998). FADD: essential for embryo development and signaling from some, but not all, inducers of apoptosis. Science *279*, 1954–1958.

Zal, T., Volkmann, A., and Stockinger, B. (1994). Mechanisms of tolerance induction in major histocompatibility complex class II-restricted T cells specific for a blood-borne self-antigen. J. Exp. Med. *180*, 2089–2099.

Zhang, J., Cado, D., Chen, A., Kabra, N.H., and Winoto, A. (1998). Fas-mediated apoptosis and activation-induced T-cell proliferation are defective in mice lacking FADD/Mort1. Nature *392*, 296–300.

Zhang, H., Zhou, X., McQuade, T., Li, J., Chan, F.K., and Zhang, J. (2011). Functional complementation between FADD and RIP1 in embryos and lymphocytes. Nature *471*, 373–376.